Responses to the comments of Reviewer 1

We, the authors, would like to extend our sincere gratitude to the reviewer for their valuable time and efforts invested in reading the manuscript. We appreciate and acknowledge all the comments, feedback, and constructive suggestions provided for the further improvement of the manuscript by the reviewer. We have tried to respond to each of the comments with the best possible clarifications, while considering the feedback, and have attempted to carefully incorporate the suggestions given by the reviewer. The responses to each of the specific comments and the corresponding figures for the clarifications are compiled below. The figure numbers are given as per the sequence of appearance of the figures in this file.

SPECIFIC COMMENTS

1. *The title: Basin formation and evolution is attributed to the combined effects of all the sublithospheric actions including underplating as well as the lithospheric plate actions and the supergene action of the lithosphere itself as expressed in all the processes that take place on the earth's surface. The title, as it is and at a glance, seems to carry the idea that underplating alone can play a significant role in basin formation.*

   Response: We agree with the reviewer, and we want to clarify here that the title used for this manuscript indicates that the magmatic underplating that has been inferred in this study is a piece of evidence that can be associated with the rift basin formation. However, we have not mentioned it as the sole mechanism for the rift formation.

2. *The authors have not shown the locations of the two basins. What they show on the map is the lithostratigraphic units bearing the names of the two basins.*

   Response: Thank you for highlighting the issue. Accordingly, Figure 1 has been modified and the location of the Vindhyan basin is now shown in Figure 1a. Rocks belonging to the Bijawar basin now form the base of the Vindhyan basin (Basu and Bickford, 2015; Mishra, 2015) and only parts of its rock sequences are exposed along the southern margin of the Bundelkhand craton (Fig. 1b). Hence, the exposures of the Bijawar supergroup, that belong to the respective basin are now shown in the geological map of Figure 1a-b.

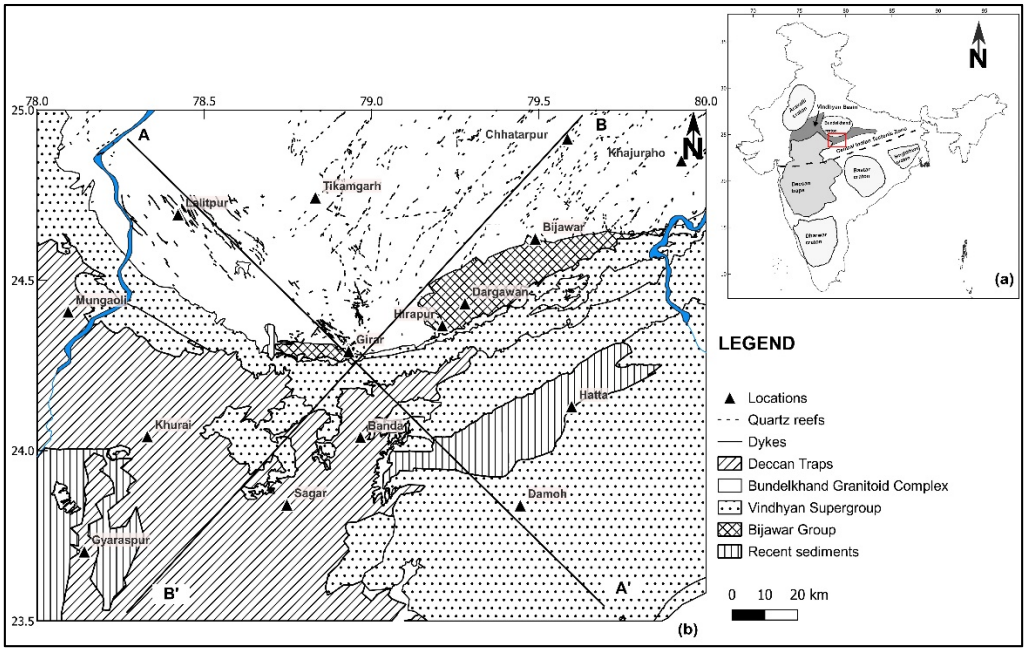

Figure 1: (a) Position of the Bundelkhand craton and Vindhyan basin with respect to other major cratons of the Indian subcontinent. Bijawar basin forms the base of the Vindhyan basin and the exposed sequences are shown in Figure 1b. (b) General geological setup of the region used for the regional scale study of the craton and surrounding areas along the southern boundary of the craton. The two profiles used for gravity modelling are marked here as AA′ and BB′.

3. *What is the rationale for upward continuing the gravity data to a 30 km height? It is more reasonable to base the continuation height on the corresponding depth estimates obtained from the radially averaged power spectrum.*

Response: The choice of the upward continuing heights was based on a trial-and-error approach as suggested by Gupta and Ramani (1980). Based on this, the 30 km upward continued regional anomaly showed some similarities with the overall trend observed in the Bouguer anomaly map (Fig. 2, below). Corresponding residual anomaly obtained after removing the 30 km upward continued regional anomaly also showed some correlations with the lithological units observed in Figure 1b. As a result, these maps were only included in the manuscript. We have utilized these results to qualitatively understand the continuation of the high-density sources at different depth levels.

We agree with the reviewer's point that it is theoretically more reasonable to consider the upward continuation height as twice the value of the source depth (Jacobsen, 1987; Meng et al., 2009; Pal and Kumar, 2019; Kebede et al., 2020). Thus, following the reviewer's suggestion, we have now included the results based on the upward continuation heights of 60 km, 30 km, and 10 km (Figs. 3A, 3B, 3C, respectively, see below) corresponding to the depth estimates from radially averaged power spectrum analysis, i.e., ~30.3 km, ~11.9 km, and ~2.7 km, respectively. The 60

km, 30 km, and 10 km upward continued regional anomalies, all showing highs occurring in the SW corner (Figs. 3A(a), 3B(a), and 3C(a), respectively). The regional and residual anomaly maps obtained by the 10 km upward continuation method (Fig. 3C) show similarity to those obtained from the 30 km upward continuation method (Fig. 3B). These suggest the continuation of high-density sources from deeper to shallower depths. Based on the geological setup of this region and the above observations, it can be inferred that the upwelling magma and eventual magmatic emplacement as an underplated layer at the lower crustal levels as well as the volcanogenic rock sequences of the Bijawar group at shallower depth (Mishra, 2015) may have caused such anomaly pattern.

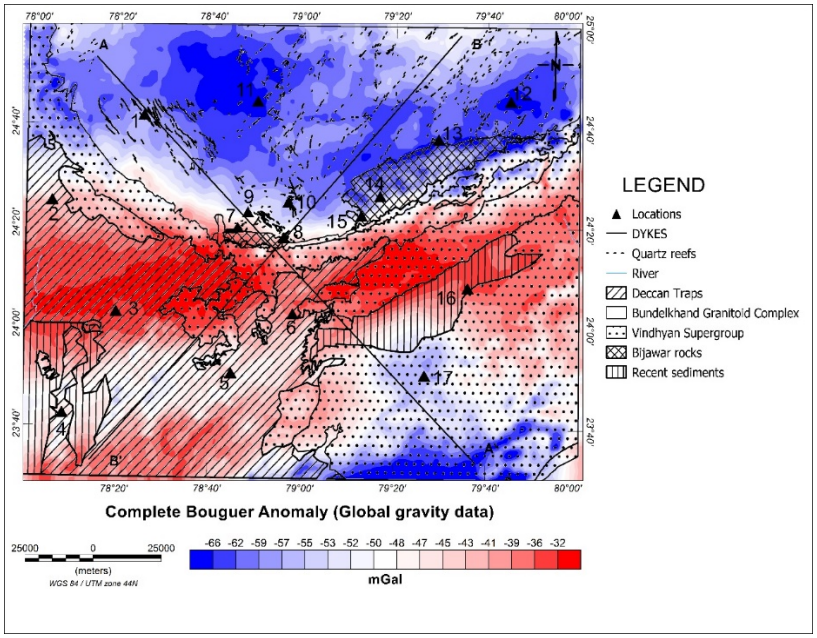

Figure 2: Complete Bouguer anomaly map (lithology map from Fig. 1 superimposed) obtained using topography and gravity data from global 1-minute topography and free-air gravity grids available on the website of the Scripps Institution of Oceanography, (https://topex.ucsd.edu/WWW_html/mar_topo.html; https://topex.ucsd.edu/cgi-bin/get_data.cgi). Locations: (1)Lalitpur, (2)Mungaoli, (3)Khurai, (4)Gyaraspur, (5)Sagar, (6)Banda, (7)Sonrai, (8)Girar, (9)Madawara, (10)Karitoran, (11)Tikamgarh, (12)Chhatarpur, (13)Bijawar, (14)Dargawan, (15)Hirapur, (16)Hatta, (17)Damoh.

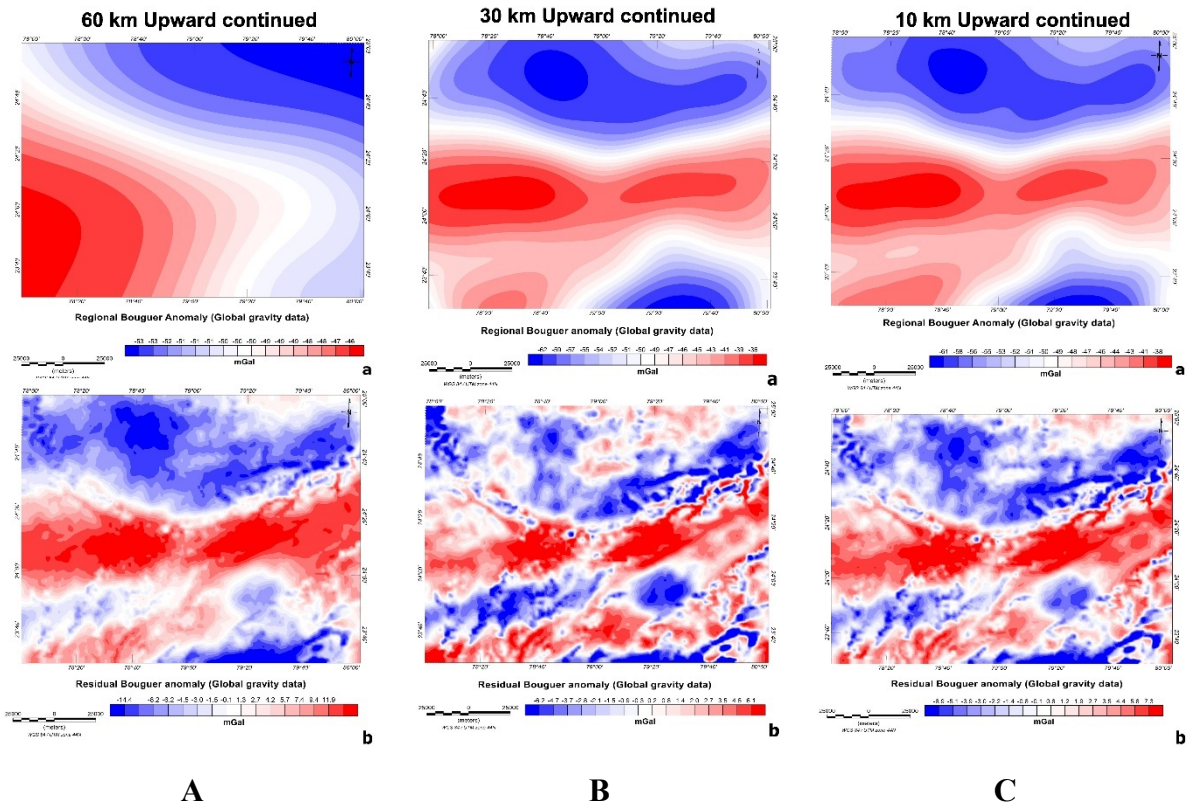

Figure 3: A. (a) Regional Bouguer anomaly map of the global gravity data, upward continued up to 60 km, (b) Residual Bouguer anomaly map of the global grid data, obtained after subtracting the 60 km upward continued regional anomaly from complete Bouguer anomaly. B. (a) Regional Bouguer anomaly map of the global gravity data, upward continued up to 30 km, (b) Residual Bouguer anomaly map of the global grid data, obtained after subtracting the 30 km upward continued regional anomaly from complete Bouguer anomaly. C. (a) Regional Bouguer anomaly map of the global gravity data, upward continued up to 10 km, (b) Residual Bouguer anomaly map of the global grid data, obtained after subtracting the 10 km upward continued regional anomaly from complete Bouguer anomaly.

4. *Gravity modelling is loosely constrained with only limited information. Hence the modeling result should be interpreted with caution.*

   Response: We agree with the reviewer's observation that gravity modelling is constrained with only limited information. This is due to the non-availability of adequate studies over the present study area along the southern margin of Bundelkhand craton. There exist few geophysical studies (Kumar et al., 2012; Gokarn et al., 2013; Mishra, 2015) on the Bundelkhand craton. These studies suggested plume/superplume setting was responsible for the formation of the Proterozoic basins of this region and even proposed the existence of an underplated mafic layer below the basins. However, a detailed subsurface model depicting the spatial and depth extent of the underplated layer based on geophysical observation and understanding its correlation with the

development of the Proterozoic basins along the southern margin of the Bundelkhand craton and adjoining areas are not available in the literature. As a result, constraints for the gravity modelling are limited and we have utilized the layering information based on the present radially average power spectra analysis as well as incorporated all the available information related to the rock types, and layer thickness as described below.

In the present modelling, the thicknesses for the different layers are majorly constrained by the results from the studies conducted using wide-angle seismic data along the Hirapur-Mandla profile by Sain et al. (2000) and the shear velocity structure given by Kumar et al. (2012), along with the depths as obtained from the radially averaged power spectrum. Best attempts have been made to carefully stick to the prior established density and thickness estimates as mentioned in Table 1. The density and thickness of the underplated layer are modified and adjusted by a trial-and-error approach to fit the gravity response curve, keeping the error between the calculated and observed gravity response as low as possible. The Moho depth for the Sagar station (~44km) suggested by Kumar et al. (2012) has been used as a constraint for the region where the underplated layer is modelled. All these details related to the constraints used for gravity modelling are already described in the section '3.5 Two-dimension forward gravity modelling'.

Table 1: Density values used in the present study, compiled from established literature.

Layers	Density (g/cm^3)	References
Recent sediments	2.1	Prasad et al. (2018)
Vindhyan supergroup	2.5	Mishra (2015); Pal and Kumar (2019)
Bijawar basement of Vindhyan	2.84	Mishra (2015
Bundelkhand granite + basement, Upper crust (average)	2.64	Podugu et al. (2017); Pati and Singh (2020)
Deccan traps	2.85	Rao et al. (2011)
Average Middle and Lower crustal density	2.8	Rao et al. (2011); Chouhan et al. (2020)
Upper mantle	3.3	Rao et al. (2011); Chouhan et al. (2020)

5. *To generalize that the high density anomaly has sources extending from deep to shallow is an over simplification. The authors have done upward continuation to a single height and they base their conclusion on it. Try to upward continue to a height of 60 (corresponding to sources at a depth of 30 km and below) to justify presence of underplate at depths in the order of 30 km in the models. In addition, the central part of the models (central region) do not show the extension of high anomaly sources to shallower depths as shown by the residual anomaly.*

Response: We are thankful to the reviewer for pointing out this concern. We apologise for this confusion. We want to clarify here that this conclusion was not based on one upward continued map but was based on a trial-and-error approach with various UC heights as suggested by Gupta and Ramani (1980). However, the 30 km upward continued regional anomaly and associated residual maps were only included in the manuscript based on visual correlation with regional trend and local features, respectively. We have utilised these results to qualitatively understand the continuation of the high-density sources at different depth level.

We have now included all the results based on the upward continuation heights of 60 km, 30 km, and 10 km (Figs. 3A, 3B, 3C, respectively, see the figures under the response on comment # 4 above) corresponding to the depth estimates from radially averaged power spectrum analysis, i.e., ~30.3 km, ~11.9 km, and ~2.7 km, respectively. The 60 km, 30 km, and 10 km upward continued regional anomalies, all showing highs occurring in the SW corner (Figs. 3A(a), 3B(a), and 3C(a), respectively). The regional and residual anomaly maps obtained by the 10 km upward continuation method (Fig. 3C) show similarity to those obtained from the 30 km upward continuation method (Fig. 3B). We have also provided the results obtained from the upward continuation up to 40 km and 50 km heights to further validate the statement referred to in the comment (Figs. 4A and 4B, see below). The centrally located high gravity anomaly, as seen for both 40 km and 50 km upward continued regional anomalies, exhibits that the high gravity signatures due to high-density material are observed at depths shallower than 30 km. These suggest the continuation of high-density sources from deeper to shallower depths. This implies that the higher gravity anomalies in the central and southwestern regions, as observed in the regional as well as residual anomalies obtained from upward continuation heights of 60 km, 50 km, 40 km, 30 km, and 10 km, are due to sources at deeper and shallower depths (Figs. 3, 4). Based on the geological set up of this region and above observations, it can be inferred that the upwelling magma and eventual

magmatic emplacement as underplated layer at shallower depth may have caused such anomaly pattern.

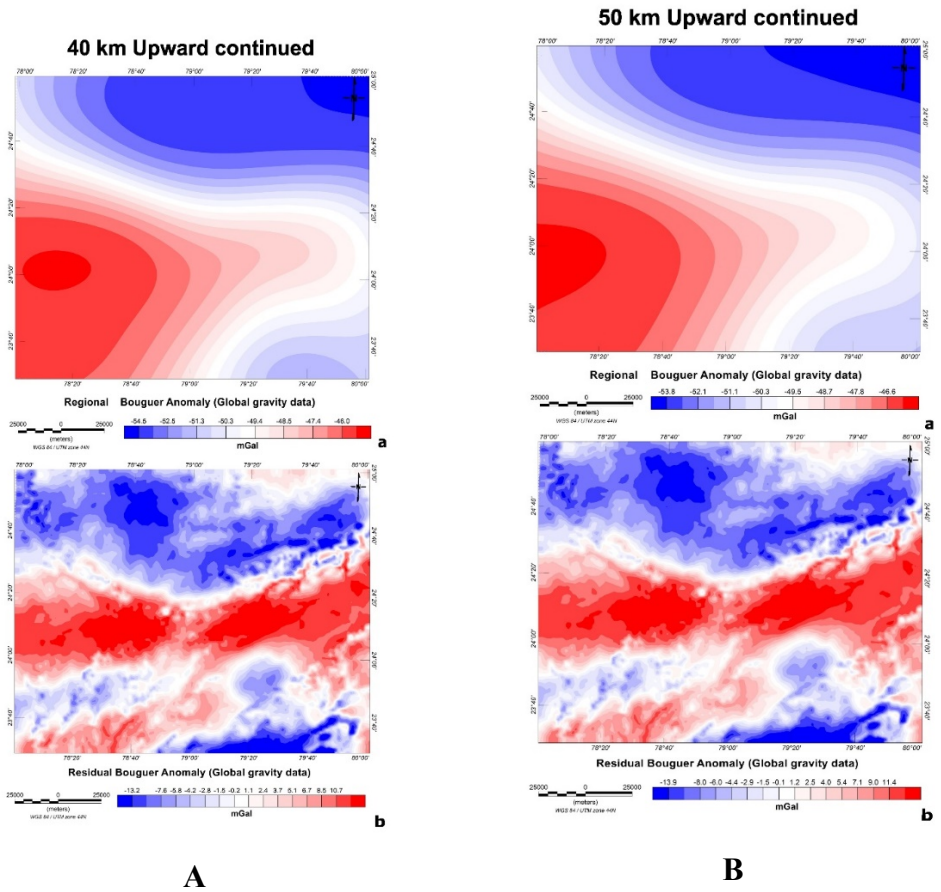

Figure 4: A. (a) Regional Bouguer anomaly map of the global gravity data, upward continued up to 40 km, (b) Residual Bouguer anomaly map of the global grid data, obtained after subtracting the 40 km upward continued regional anomaly from complete Bouguer anomaly. B. (a) Regional Bouguer anomaly map of the global gravity data, upward continued up to 50 km, (b) Residual Bouguer anomaly map of the global grid data, obtained after subtracting the 50 km upward continued regional anomaly from complete Bouguer anomaly.

6. *On Line 332 the paper asserts that there is **striking** similarity between the inverted Moho topography and the gravity signature. Please tone down this assertion. There is similarity but pay attention to the following remarks: a. the gravity anomaly from the inverted Moho topography shows a slightly southward shift and centered at the southern margin of the regional anomaly. b. at the southwestern corner the effect is in fact opposite. There is high anomaly in the both the regional and residual gravity but low anomaly in the gravity obtained from the Moho.*

Response: We are thankful to the reviewer for raising this concern as it helped us to remove the confusion. We agree with the reviewer's observation on figures 5b and 3a

of the manuscript. However, these two figures are generated based on two different mathematical concepts but still show significant similarities in terms of anomaly trend and overall pattern. These converging results provide confidence in the interpretation. Maybe we were too optimistic about this, however, as per the suggestion of the reviewer the statement has been toned down.

We also want to mention here that Figures 5b and 3a (of the manuscript) had different areal coverage as the Parker-Oldenburg inversion scheme (used for Figure 5b of the manuscript) required square shaped area. As a result, the latitudinal extent of the data used for Figure 5b (of the manuscript) was 23°–25° N but that for the present study area is 23.5°–25° N. This might have resulted in the observation of point *b* in the comment. To avoid any confusion, the new figure (Fig. 5a, see below) corresponding to the results of the inversion method has the study area marked by a red box, and the colour map format for both figures is now kept as same. The E-W trending high gravity in both inversion results (Fig. 5a) and 30 km upward continued regional anomaly (Fig. 5b, see below) shows a general similarity in the trend.

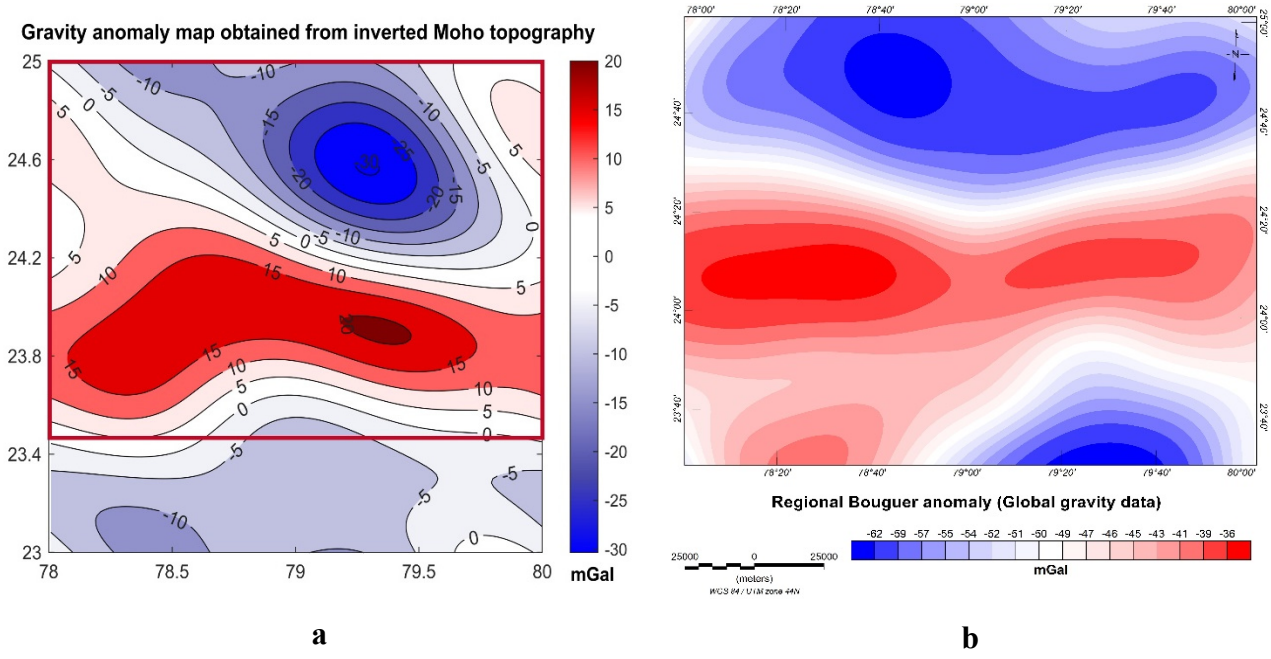

Figure 5: (a) Gravity map obtained using the inverted Moho topography obtained from Parker-Oldenburg algorithm. The red box marks the study area as seen in the adjacent regional anomaly map. (b) Regional Bouguer anomaly map of the global gravity data upward continued up to 30 km.

7. *I have serious reservation on the contradictory results obtained from the two approaches of the gravity modeling. The authors obtained the undulation of the Moho interface using the downward continuation formula as given by the modification of Parker-Oldenburg algorithm (Fig. 5a). As is also noted by the authors the Moho depth undulations obtained by this method beneath the basins where underplate is observed do not correspond to the depths obtained by forward modeling (Fig. 6 & 7). The underplate top is considered as Moho in Fig. 5a whereas the underplate bottom is considered as Moho in both Fig. 6 & 7. In addition, there is also a clear discrepancy in areas where there is no underplate. Compare, for example, Fig. 5a with Fig. 7. In northeast where there is no underplate the Moho depth varies between 37 and 39 km in the forward model in Fig. 7 whereas in Fig. 5a the depth variation for the same area is between 33 and 44 km. These contradictions should not have occurred since there is a clear density contrast between the mantle and the underplate and the Parker-Oldenburg approach is capable of recognizing the difference between them.*

   Response: We acknowledge the observation made by the reviewer. The average crustal density value of 2.78 g/cm^3 is obtained by taking the average densities of the crustal layers corresponding to the Vindhyan sequences, Bijawar group, average density of Upper crust (Bundelkhand granite + basement), average density of middle and lower crust as well as the underplating (all these densities are mentioned in Table 1 of the manuscript as well as in the response for comment #4 above). The density contrast then obtained with the mantle (i.e., 0.52 g/cm^3) was used for the inversion (Fig. 6A, see below). The Parker-Oldenburg method is also applied using a density contrast of 0.6 g/cm^3 (Fig. 6B, see below) using the average crustal density eliminating the underplating density. The results (Fig. 6A & 6B) follow similar trends as the results shown in the manuscript, and the Moho values in the central region (below the Vindhyan rocks) show a range of values from 32 km to 36 km. Thus, we observed that a density difference of 0.15 g/cm^3 between the underplated layer and mantle is not very distinctly observed in Moho depth variations, irrespective of whether the underplated layer is included in the average crustal density calculations or not. As the inversion results are unable to distinguish the underplated layers, the obtained Moho depths appear shallower in the Parker-Oldenburg inversion method. This can be also observed in the Distance vs. Moho depth plot using the inverted Moho topography (as obtained from Parker-Oldenburg inversion method) along with the Moho depth with and without the thickness of underplated layers as obtained from forward models (Figs. 7A and 7B,

below) below the profiles AA′ and BB′. These plots show that the general trend of the underplating interface from the forward model and the trend of the Moho structure from the inversion results along the profiles AA′ (Fig. 7A) and BB′ (Fig. 7B) exhibit similarity. Thus, the inversion scheme is unable to distinguish the underplated layer from the Moho depth level unlike the forward modeling scheme. This may have resulted in apparent contradiction as pointed by the reviewer but that is the limitation of the inversion scheme.

Therefore, we have developed the better constrained forward models along two profiles by considering the initial models based on a combination of the results of RAPS analysis, inverted Moho topography, and the crustal layer thicknesses obtained from prior literature (as mentioned in the response for comment #4). The discrepancy pointed out in the Moho depths for the regions not exhibiting the underplating in the forward models (e.g. below the Bundelkhand craton) is possibly observed as they have been constructed by adjusting the layer thicknesses, and depths according to the above-mentioned constraints. The Moho depth ranges for regions covered by the Bundelkhand craton and the Vindhyan basin as suggested by Kumar et al. (2012) have been used as a constraint for the region of the modelled underplated layer, which varies from ~36 km to ~44 km. These depth ranges were used as constraints with a trial-and-error approach for the forward modelling while keeping the density values consistent with the density contrast utilized for the inversion method. Therefore, the forward models represent more refined and better-constrained results which follow the broad trend of inversion results.

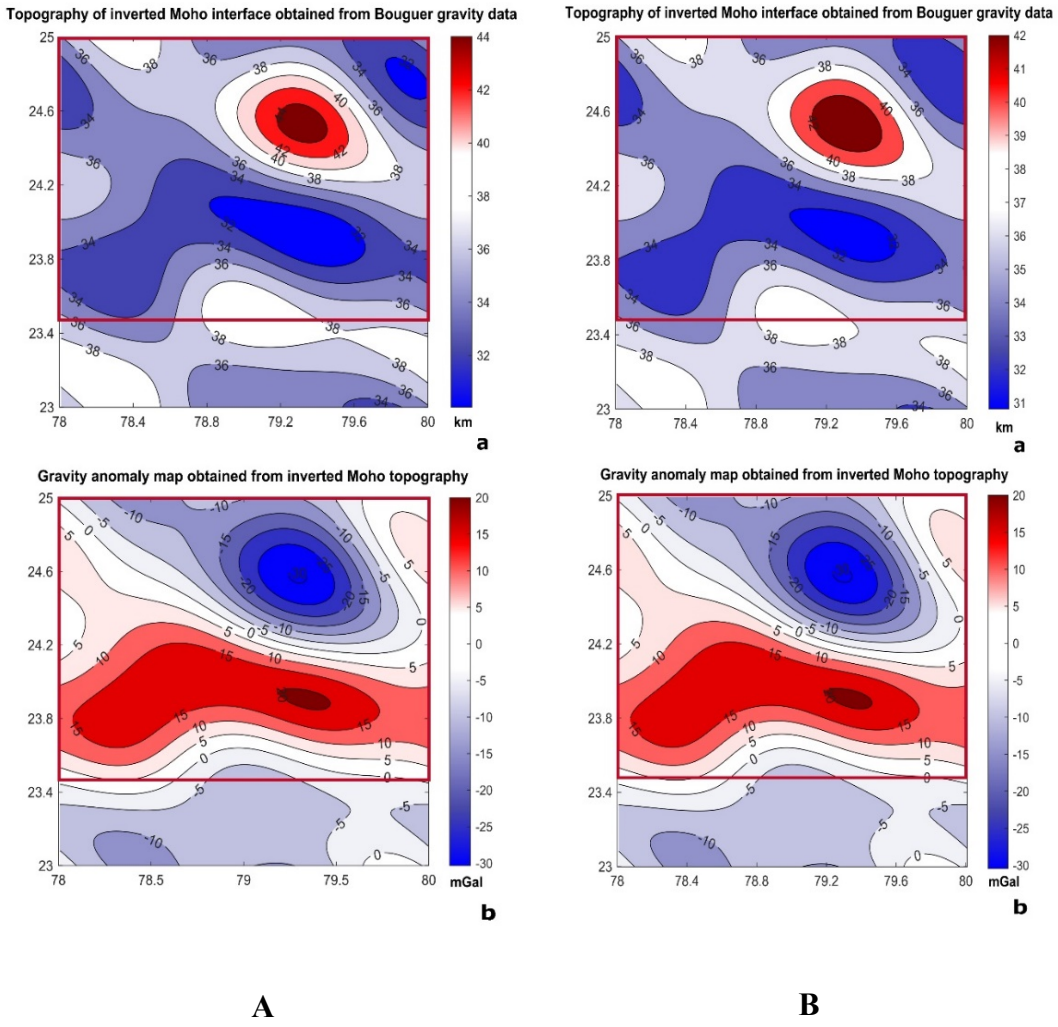

Figure 6: A. (a) Moho topography map obtained by applying the Parker-Oldenburg method on the Bouguer gravity data of Fig. 2, using 0.52 g/cm^3 as the density contrast. (b) Gravity map obtained using the inverted Moho depths from Fig. 6A(a). The red box marks the study area. B. (a) Moho topography map obtained by applying the Parker-Oldenburg method on the Bouguer gravity data of Fig. 2, using 0.6 g/cm^3 as the density contrast. (b) Gravity map obtained using the inverted Moho depths from Fig. 6B(a). The red box marks the study area.

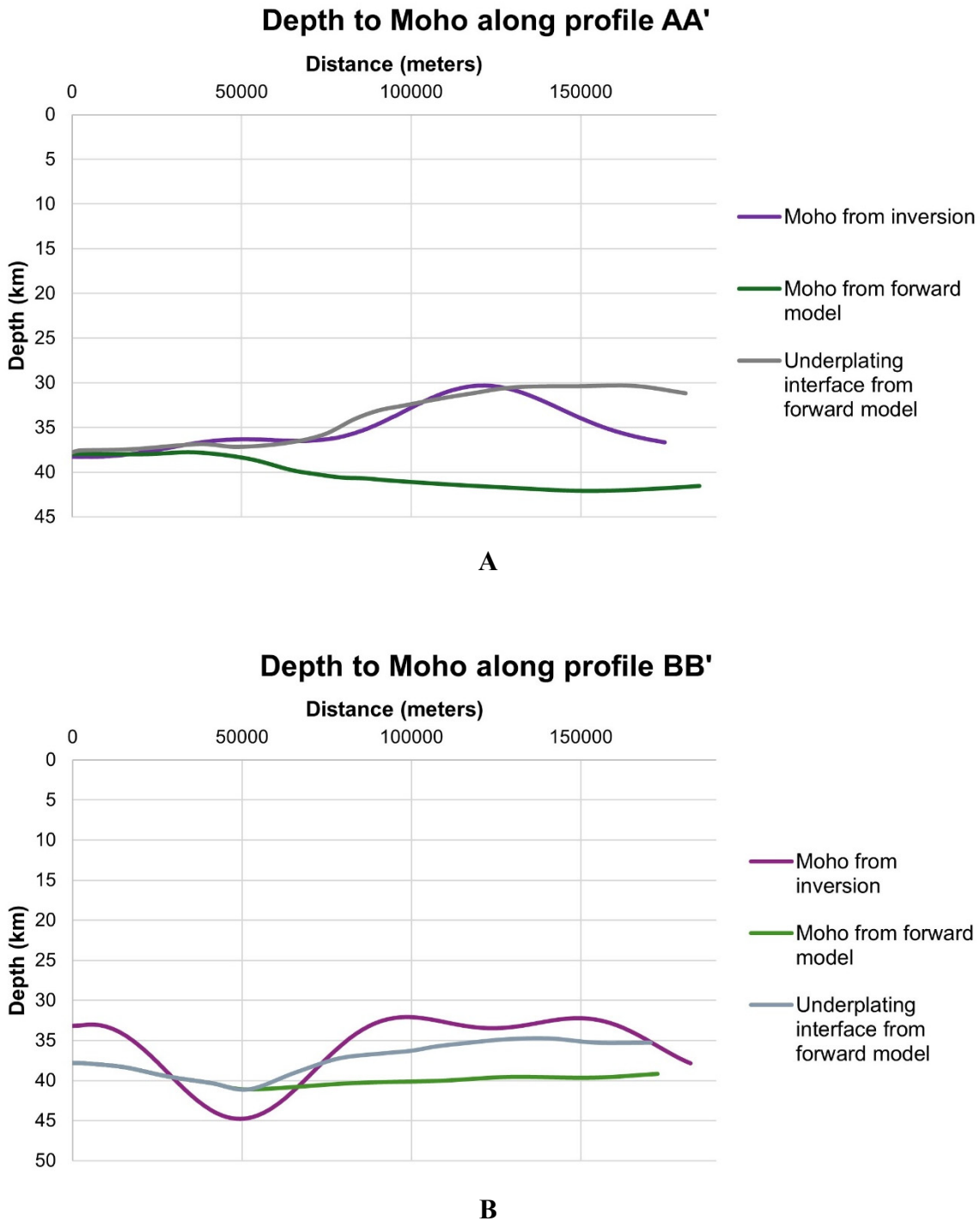

Figure 7: (A) Distance vs. Moho depth plot using the inverted Moho topography, Moho interface from the forward model, and underplating interface from the forward model along the profile AA'. (B) Distance vs. Moho depth plot using the inverted Moho topography, Moho interface from the forward model, and underplating interface from the forward model along the profile BB'

TECHNICAL CORRECTIONS

Response: The below-mentioned changes have been made in the manuscript.

- On Line 29 "…..attributed to the presence of underplated layers, like rift basins…" Please remove the word "like".
- On Lines 194 and 197- 8 the phrase h(x) and z_o are redundant. Please eliminate the repetition.
- On Line 346 it must be "crustal uplift" and not "crustal upliftment".
- In Fig. 5 contour values can be indicated on every other line to avoid congestion.

REFERENCES

Basu, A. and Bickford, M. E. An alternate perspective on the opening and closing of the intracratonic Purana basins in peninsular India, Journal of Geological Society of India 85(1), 5–25, 2015.

Gupta, V. K., and Ramani, N. Some aspects of regional-residual separation of gravity anomalies in a Precambrian terrain. Geophysics 45: 1412-1426, 1980.

Jacobsen, B.H. Case for upward continuation as a standard separation filter for potential-field potential-field maps. Geophysics 52, 1138–1148, 1987.

Kebede, H., Alemu, A., Fisseha, S. Upward continuation and polynomial trend analysis as a gravity data decomposition, case study at Ziway-Shala basin, central Main Ethiopian rift. Heliyon, 6, 2020.

Kumar, T. V., Jagadeesh, S., and Rai, S.S.: Crustal structure beneath the Archean–Proterozoic terrain of north India from receiver function modelling, Journal of Asian Earth Sciences 58, 108–118, 2012.

Meng, X., Guo, L., Chen, Z. Shuling, L., and Lei, Shi. A method for gravity anomaly separation based on preferential continuation and its application. Appl. Geophys. 6, 217–225 2009.

Mishra, D. C.: Plume and Plate Tectonics Model for Formation of some Proterozoic Basins of India along Contemporary Mobile Belts: Mahakoshal — Bijawar, Vindhyan and Cuddapah Basins, Journal of the Geological Society of India 85(5), 525–536, 2015.

Oasis Montaj MAGMAP manual: http://updates.geosoft. com/downloads/Bles/how-to-guides/Getting˙Started˙with˙ montaj˙MAGMAP˙Filtering.pdf.

Pal, S. K. and Kumar, S.: Subsurface Structural Mapping using EIGEN6C4 Data over Bundelkhand Craton and Surroundings: An Appraisal on Kimberlite/lamproite Emplacement. Journal of the Geological Society of India, 94(2), 188–196, 2019.

Sain, K., Bruguier, N., Murty, A. S. N., and Reddy, P. R.: Shallow velocity structure along the Hirapur-Mandla profile using travel time inversion of wide-angle seismic data, and its tectonic implications. Geophysical Journal International 142(2), 505–515, 2000.